Dispersion of the volcanic sulfate cloud from a Mount Pinatubo–like eruption

Valentina Aquila,[1] Luke D. Oman,[1] Richard S. Stolarski,[1,2] Peter R. Colarco,[1] and Paul A. Newman[1]

Received 3 October 2011; revised 25 January 2012; accepted 26 January 2012; published 29 March 2012.

[1] We use the GEOS-5 general circulation model to simulate the transport of the volcanic cloud from an eruption similar to the 1991 eruption of Mount Pinatubo. The simulated aerosol optical thickness and transport of the volcanic cloud are in good agreement with observations of the actual Pinatubo eruption from the Stratospheric Aerosol and Gas Experiment II (SAGE II) and the Advanced Very High Resolution Radiometer (AVHRR) and with vertical profiles of sulfur dioxide observed by the Microwave Limb Sounder (MLS). We tested the importance of initial conditions corresponding to the specific meteorological situation at the time of the eruption by comparing results when GEOS-5 is initialized using Modern Era Retrospective Analyses for Research and Applications (MERRA) reanalysis fields with results when it is initialized from an existing model run. We found no significant difference in the transport of the cloud. We show how the inclusion of the interaction between volcanic sulfate aerosol and radiation is essential for a reliable simulation of the transport of the volcanic cloud. The absorption of longwave radiation by the volcanic sulfate largely induces the rising of the volcanic cloud up to the middle stratosphere and the divergent motion from the latitude of the eruption to the tropics. Our simulations indicate that the cloud is transported to the Northern Hemisphere through a lower stratospheric pathway and to middle and high latitudes of the Southern Hemisphere through a middle stratospheric pathway, centered at about 30 hPa. The direction of the middle stratospheric pathway depends on the season of the eruption.

Citation: Aquila, V., L. D. Oman, R. S. Stolarski, P. R. Colarco, and P. A. Newman (2012), Dispersion of the volcanic sulfate cloud from a Mount Pinatubo–like eruption, *J. Geophys. Res.*, *117*, D06216, doi:10.1029/2011JD016968.

1. Introduction

[2] Volcanic eruptions are a major source of stratospheric aerosol [*Deshler*, 2008]. Sulfur dioxide (SO_2) injected into the stratosphere by large eruptions is oxidized into sulfate aerosol and can increase the background aerosol mass by orders of magnitude. The induced perturbation of the stratospheric aerosol layer can persist for a few years. During such time the aerosol from a tropical eruption can spread over the whole globe, changing the global climate in a significant way [*Robock*, 2000].

[3] Mount Pinatubo is located in the Philippines (15.1°N, 120.4°E). Pinatubo erupted on 15 June 1991, injecting about 20 Tg of SO_2 into the atmosphere [*Bluth et al.*, 1992]. The resulting sulfate cloud was detected at altitudes higher than 30 km [*McCormick and Veiga*, 1992]. After about 1 year, roughly one third of the volcanic aerosol was still present in the atmosphere. The sulfate cloud generated by the eruption of Mount Pinatubo circled the globe and crossed the equator within 3 weeks of the eruption [*Guo et al.*, 2004; *McCormick and Veiga*, 1992] and diffused to middle and high latitudes in both the Northern and the Southern hemispheres.

[4] Such broad meridional spreading is not typical of all tropical eruptions. The volcanic cloud from the April 1982 El Chichón eruption, located 2° north of Mount Pinatubo, was mainly confined to the Northern Hemisphere [*McCormick and Swissler*, 1983]. *Young et al.* [1994] first suggested that the cross-equatorial transport of the Mount Pinatubo cloud was due to local absorption of infrared radiation from the troposphere. *Timmreck et al.* [1999a] showed this hypothesis was plausible with a one-simulation study using the MAECHAM4 Hamburg climate model. *Niemeier et al.* [2009] applied the most recent version of the MAECHAM5 Hamburg climate model, coupled to an aerosol microphysical model, to the study of the Pinatubo eruption, showing that the radiative heating of the aerosol has a strong impact on the behavior of the volcanic cloud. *Stenchikov et al.* [1998] and *Kirchner et al.* [1999] showed that the absorption of near-IR radiation by the volcanic aerosol contributes significantly to the stratospheric heating. *Thomas et al.* [2009] showed by means of simulations with prescribed aerosol distributions that the phase of the quasi-biennial oscillation (QBO) at the moment of the eruption can produce a large stratospheric temperature response.

[1]Laboratory for Atmospheric Chemistry and Dynamics, NASA Goddard Space Flight Center, Greenbelt, Maryland, USA.
[2]Department of Earth and Planetary Sciences, Johns Hopkins University, Baltimore, Maryland, USA.

0148-0227/12/2011JD016968

Table 1. List of Performed Experiments

Name	Injected SO_2 (Tg)	Injection Height (km)	Eruption Date	Radiatively Interactive Aerosol	Ensemble Members
REF	20	16–18	15 June 1991	Yes	8
CONTROL	20	16–18	15 June 1991	No	8
CONTROL-HIGH	20	17–27	15 June 1991	No	3
0.25REF	5	16–18	15 June 1991	Yes	3
0.25REF-HIGH	5	17–27	15 June 1991	Yes	3
WINTER	20	16–18	15 January 1991	Yes	3
SPRING	20	16–18	4 April 1991	Yes	3

[5] It is still unclear if the eruption of Mount Pinatubo modified the circulation in the Southern Hemisphere. *Robock et al.* [2007] identified no significant anomaly in the Southern Hemisphere circulation in their simulations with the NASA/GISS ModelE general circulation model. In contrast, *Karpechko et al.* [2010], *Marshall* [2003], *Roscoe and Haigh* [2007], and *Crooks and Gray* [2005] found a negative response of the Southern Annular Mode in both models and observations.

[6] In this paper, we simulate a Mount Pinatubo–like eruption and the dispersal of the subsequent sulfate cloud with the free-running Goddard Earth Observing System (GEOS-5) general circulation model [*Rienecker et al.*, 2008], coupled to the GOCART aerosol transport module [*Colarco et al.*, 2010] and a stratospheric chemistry module [*Pawson et al.*, 2008]. GEOS-5 is here for the first time applied to the simulation of stratospheric volcanic aerosol. An eruption as large as the Mount Pinatubo eruption represents a significant perturbation of the atmosphere radiative balance and might induce changes in the stratospheric dynamics. In this work we investigate the dynamical response of the stratosphere to an injection of sulfate aerosol due to a Pinatubo-like eruption, focusing on the first 6 months after the eruption. We show that the absorption of longwave radiation by the volcanic sulfate cloud largely determines the transport of the cloud itself. We do not simulate the effect of the QBO on the transport of the volcanic cloud.

[7] In section 2, we describe the model and the modifications introduced to simulate stratospheric volcanic aerosol. In section 3, we present the model results and the comparison with observations of aerosol optical thickness (AOT) from the Stratospheric Aerosol and Gas Experiment II (SAGE II) and the Advanced Very High Resolution Radiometer (AVHRR), and with vertical profiles of SO_2 observed by the Microwave Limb Sounder (MLS). In section 4 we show how the inclusion of a radiative interactive volcanic aerosol is essential for a reliable simulation of the dispersal of the Mount Pinatubo volcanic cloud. We calculate the perturbation of background stratospheric winds and show the results of the simulation of a volcanic eruption of magnitude equal to one fourth of a Pinatubo-like eruption. Finally, in section 5 we present two experiments to investigate the effects of the season of the eruption on the transport of the volcanic cloud. Table 1 lists the experiments included in this work.

2. The GEOS-5 General Circulation Model

[8] All simulations presented in this study are performed with the Goddard Earth Observing System, Version 5 (GEOS-5) model [*Rienecker et al.*, 2008], a system of component models integrated using the Earth System Modeling Framework (ESMF).

[9] The GEOS-5 atmospheric general circulation model (AGCM) is able to perform weather and climate simulations used for atmospheric analyses, weather forecasts and climate simulations and predictions. GEOS-5 uses a finite volume dynamical core [*Lin*, 2004] combined with a physics package that describes moist processes, radiation, turbulent mixing and surface processes. Convection is parameterized using the relaxed Arakawa-Schubert (RAS) scheme [*Moorthi and Suarez*, 1992], and is combined with a prognostic cloud scheme. The boundary layer turbulent mixing is parameterized with the schemes by *Louis et al.* [1982] and *Lock et al.* [2000] for stable and unstable situations, respectively. The land surface model is composed of a catchment-based hydrological model [*Koster et al.*, 2000] and a multilayer snow model [*Stieglitz et al.*, 2001]. The radiative transfer model consists of a solar radiation model [*Chou and Suarez*, 1999] and a thermal radiation model [*Chou et al.*, 2001]. The solar radiation model includes absorption due to water vapor, O_3, O_2, CO_2, clouds and aerosols. The thermal radiation model includes absorption by water vapor, CO_2, O_3 and most of the minor trace gases, as well as clouds and aerosols.

[10] GEOS-5 additionally contains modules for chemistry and aerosols. Coupled chemistry-climate simulations are performed using a module for stratospheric chemistry [*Pawson et al.*, 2008]. The aerosol transport module is based on the Goddard Chemistry, Aerosol, Radiation and Transport (GOCART) model [*Chin et al.*, 2000, 2002]. An online version of GOCART in the GEOS modeling system is described and evaluated by *Colarco et al.* [2010]. GOCART includes a parameterization of the chemical production of SO_4 aerosol from oxidation of dimethyl sulfide (DMS) by OH during day and NO_3 during night, and from oxidation of SO_2 by OH in the gas phase and by H_2O_2 in the aqueous phase. In this study we only consider SO_2 injections from our Mount Pinatubo–like source and neglect other aerosols besides sulfate (e.g., dust, sea salt, and carbonaceous aerosols).

[11] We modify GOCART to include the gravitational settling of sulfate in order to properly simulate stratospheric volcanic aerosol. The settling velocity is a function of the particle's wet radius. The sulfate growth factor β_{SO4} is calculated as a function of the relative humidity RH following *Petters and Kreidenweis* [2007] as

$$\beta_{SO_4} = \frac{r_{wet}}{r_{dry}} = \sqrt[3]{\frac{RH(1-k)-1}{RH-1}},$$

Table 2. SO_2 and SO_4 *e*-Folding Time of Each Ensemble Member of Experiment REF and Average Values and Standard Deviation of the Ensemble

	e-Folding Time	
Ensemble Member	SO_2	SO_4
1	31	373
2	29	340
3	26	243
4	34	426
5	29	372
6	29	345
7	26	275
8	34	402
Average	29.8	347
Standard deviation	2.9	57.7

where the hygroscopic parameter k is equal to 1.19 and r_{dry} is the dry effective radius, which is a tuning parameter. We performed several sensitivity tests varying the value of the sulfate dry radius. Assuming a lognormal unimodal distribution, the median radius r_m and the effective radius r_e are related through the equation

$$r_e = r_m \ \exp\left[\frac{5}{2}\ln^2\sigma\right],$$

where σ is the standard deviation of the lognormal distribution. In this work we assume that the aerosol is lognormally distributed with median radius equal to 0.35 μm and standard deviation 1.25. This corresponds to an effective dry radius equal to 0.40 μm. The chosen median radius is within the range of observed values for sulfate aerosol from Mount Pinatubo [e.g., *Bingen et al.*, 2004; *Russell et al.*, 1996; *Stenchikov et al.*, 1998], and results in good agreement with the AOT retrieved by SAGE II and AVHRR (section 3.1). The simulated total mass of sulfate is reduced by a factor *e* in about 1 year (Table 2), in agreement with observations [*McCormick et al.*, 1995].

[12] GEOS-5 can run with radiatively interactive aerosol, which means that the aerosol concentrations simulated by GOCART can modify the meteorological fields. The simulations shown in section 3 are performed with radiatively interactive aerosol, if not otherwise specified. Some results from runs with noninteractive aerosol are presented in section 4. The aerosol optical properties are read from look-up tables previously generated using the OPAC database [*Hess et al.*, 1998]. The look-up tables contain the aerosol mass scattering and extinction coefficients as a function of relative humidity and radiation wavelength. We apply Mie theory to calculate the aerosol optical properties, and assume that aerosol is lognormally distributed and externally mixed.

[13] GEOS-5 can be run both in climate or data assimilation mode. The simulations performed in this study are climate mode simulations, i.e., they provide a multiyear forecast starting from specified initial conditions. We apply GEOS-5 with resolution 2.0° latitude by 2.5° longitude. The model has 72 vertical layers in a hybrid coordinate system from surface to 0.01 hPa (~95 km). The model version used in this work does not include a simulation of the QBO, but simulates easterly winds in the tropical stratosphere, as observed at the time of the eruption in the middle stratosphere. We neglect the aerosol impact on the stratospheric chemistry.

3. Simulation of a Mount Pinatubo–Like Eruption

[14] We simulated a Pinatubo-like eruption by injecting 20 Tg of SO_2 in the grid box containing Mount Pinatubo during the day of 15 June 1991 (experiment REF). The SO_2 load is initially distributed between 16 and 18 km and is lofted to higher altitudes within the first weeks because of the model response to radiatively interacting aerosol. Other model studies [e.g., *Timmreck et al.*, 1999b; *Zhao et al.*, 1995] place the injection of SO_2 at a higher altitude, basing their assumption on SAGE II observations. At the moment of the eruption, however, SAGE II was observing at about 70°N [*Trepte et al.*, 1993], and observed at the latitude of Mount Pinatubo only 15 days after the eruption. At that stage the absorption of radiation by the volcanic aerosol had already induced the lofting of the cloud itself, as we show later.

[15] We tested different assumptions on the injection height by performing additional simulations with injection of SO_2 between 16 and 25, 17 and 27, 20 and 27, and 20 and 30 km. In all these simulations, the bulk of the volcanic cloud reached altitudes much higher than the observations. Our choice of an injection altitude between 16 and 18 km, lower than assumed by the other model studies, results in a reasonable simulation of the SAGE II vertical profile observed a couple of weeks after the eruption (section 3.2).

[16] We performed an ensemble of eight transient simulations, each spanning from January 1991 to December 1997 (experiment REF). The initial conditions of the ensemble members are the meteorological fields of eight different Januaries from a transient 8 year control simulation with no volcanic perturbation, which was initialized with climatological meteorological fields typical of the year 2000. The CONTROL experiment includes this transient control simulation and seven additional simulations, initialized with the same sets of initial conditions used for experiment REF. All the model results shown in this work are ensemble averages, if not otherwise specified.

[17] The SO_2 mass injected in our GEOS-5 simulations is reduced by a factor of *e* after 29.8 days (ensemble mean), in good agreement with observations by the Total Ozone Mapping Spectrometer (TOMS) [*Bluth et al.*, 1992; *Guo et al.*, 2004]. The simulated SO_4 is reduced by a factor of *e* in 347 days, also in good agreement with observations [*Barnes and Hofmann*, 1997; *Nagai et al.*, 2010]. Table 2 shows the *e*-folding times of SO_2 and SO_4 for each ensemble member.

[18] Figure 1 shows the temporal evolution of the globally averaged AOT at 550 nm. The results from our simulations are compared to SAGE II [*Thomason et al.*, 1997] and AVHRR [*Long and Stowe*, 1994] observations. We removed background values from the AVHRR observations, calculated as the monthly mean AOT over the available months preceeding the eruption (June 1989 to May 1991). In Figure 1 we indicate the AOT ensemble average with a solid black line, and the variability of the model with the light blue shading. The variability increases particularly starting from November 1991, as reflected also in the broad range of *e*-folding times of Table 2, but is relatively small during the

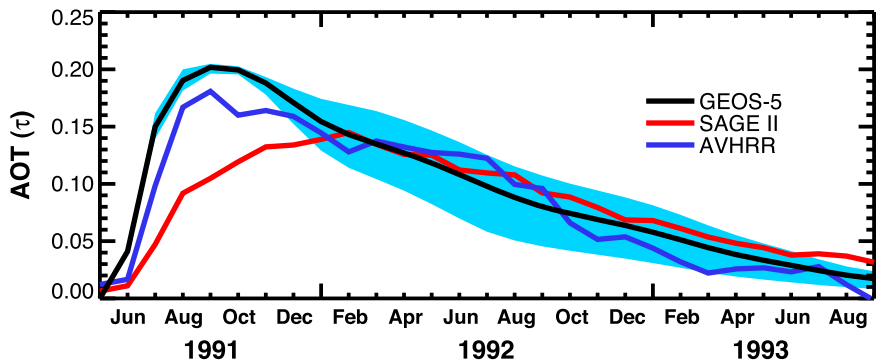

Figure 1. Global mean of the visible aerosol optical thickness as simulated by GEOS-5 (experiment REF, black line) and as derived by Stratospheric Aerosol and Gas Experiment II (SAGE II; red line), and Advanced Very High Resolution Radiometer (AVHRR; blue line) data. Background values have been removed from the AVHRR data. The blue shaded area shows the variability of the ensemble.

first 6 months after the eruption. The simulated peak value is in reasonable agreement with AVHRR, but is higher in magnitude and occurred earlier in time than the SAGE II data. Optical depths of about 0.15 or more, however, saturate the SAGE II measurement [*Russell et al.*, 1996]. Hence, the value S of AOT calculated from SAGE II observations are probably underestimated.

3.1. Horizontal Dispersion of the Volcanic Cloud

[19] Both in the observations and in our simulations, the volcanic cloud is transported northward out of the tropics and southward toward the equator shortly after the eruption. Figure 2 shows the zonal mean of the AOT, averaged over the 8 ensemble members, as a function of time, for our simulations and for the satellite observations. The model reproduces reasonably well the spreading of the cloud into the two hemispheres observed by SAGE II and AVHRR. GEOS-5 simulates well the time scale and the intensity of the tropical peak compared to AVHRR. As expected from the profiles in Figure 1, the magnitude of the simulated aerosol optical thickness is larger than the one observed by SAGE II. GEOS-5 simulates also the second peak in 1992 at 45°N. The high AOT values observed at 60°S in November 1991 might be due to the eruption of the Cerro Hudson volcano (72.97°W, 45.90°S) between August and October 1991, which is not included in our simulations. The eruption of Cerro Hudson injected about 1.5 Tg of SO_2 between 12 and 16 km [*Saxena et al.*, 1995], and created a layer of fresh aerosol particles at 15 km altitude [*Pitts and Thomason*, 1993].

[20] GEOS-5 transports a large fraction of the cloud southward shortly after the eruption, but slightly underestimates the transport across the equator with respect to the observations. While the simulated peak is located on the equator, both SAGE II and AVHRR detected the peak at about 5°S. The results by *Timmreck et al.* [1999a] also underestimated the cross-equatorial transport. They suggested that the missing transport might be due to the specific meteorological situation in June 1991, when a strong high over Tibet induced a southward transport of the cloud. We tested the importance of the specific meteorological situation by performing a simulation starting on 14 June 1991 with specified initial conditions from the Modern Era Retrospective Analyses for Research and Applications (MERRA) [*Rienecker et al.*, 2011]. Such initial conditions are derived from observational data and are therefore close to the real meteorological situation that took place in June 1991. The results (not shown) are similar to the reference simulations, with a peak of the AOT on the equator. This suggests that the detailed meteorological situation at the moment of the eruption is not responsible for the additional southward transport.

[21] The sensitivity tests that we performed with different SO_2 injection heights (16–25, 17–27, 20–27, and 20–30 km) showed very similar AOT horizontal distributions, even if the volcanic clouds reached altitudes higher than observed. The small initial underestimation of the southward transport might be due to the lack of radiatively interactive SO_2 and QBO in the version of GEOS-5 used in this work. *Lary et al.* [1994] estimated that the SO_2 heating rate can be up to 1 K/d and could therefore be significant in the early stages of the cloud's evolution. *Hitchman et al.* [1994] showed that the QBO plays an important role in the meridional distribution of stratospheric aerosol. *Trepte et al.* [1993] discussed how the phase of the QBO might have influenced the dispersal of the Mount Pinatubo volcanic cloud.

3.2. Vertical Distribution of the Volcanic Cloud

[22] We compare our results with SO_2 profiles taken with MLS onboard the Upper Atmosphere Research Satellite (UARS) between 10°S and the equator on 21 September 1991 (Figure 3) [*Read et al.*, 1993]. The simulated profile corresponds to the September 1991 monthly mean of the SO_2 vertical profiles, averaged over the latitudinal band between 10°S and 10°N. We averaged over a latitudinal band larger than the MLS observations to compensate for different latitudinal rates of transport between simulations and observations. Both the modeled and observed SO_2 profiles peak at about 20 hPa with similar magnitude. The sensitivity tests that we performed varying the injection altitude of SO_2 showed differences in the vertical profile of the volcanic cloud during the first months, but the equilibrium level where the bulk of the cloud settles was in all tests at about 20 hPa.

[23] Figure 4 shows the vertical distribution of the zonally averaged simulated SO_4 concentration (ensemble mean) on

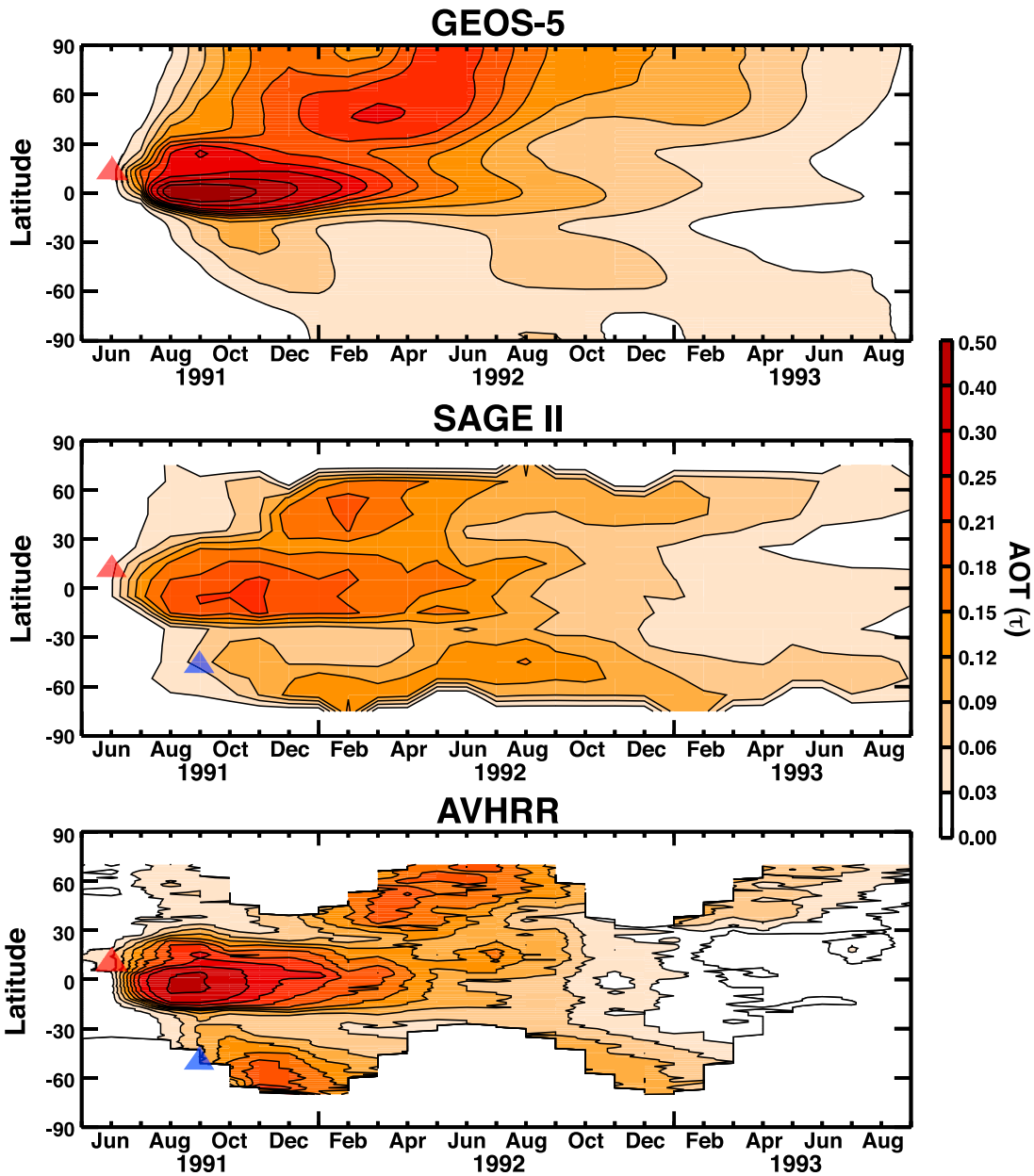

Figure 2. Zonal mean of the aerosol optical thickness at 550 nm for the Mount Pinatubo eruption in the GEOS-5 simulations (top, experiment REF), SAGE II (middle), and AVHRR (bottom) observations. Background values have been removed from the AVHRR observations. The red triangles indicate the latitude and time of the Mount Pinatubo eruption, while the blue triangles in Figures 2 (middle) and 2 (bottom) show the time and location of the Cerro Hudson eruption.

15 July, 1 September, 1 November, and 31 December 1991. The bulk of the cloud is between 50 and 20 hPa in July 1991. The model results are in agreement with SAGE II observational satellite data [e.g., *Anderson and Saxena*, 1996; *McCormick and Veiga*, 1992; *Trepte et al.*, 1993; *Vernier et al.*, 2011]. *McCormick and Veiga* [1992] detected the cloud top at altitudes up to 29 km (about 13 hPa) during June, July and August 1991. *Trepte et al.* [1993] showed the latitude-altitude cross section of the SAGE II 1 μm extinction ratio. Data were first collected in the tropical region between 1 July and 20 July, and show values higher than the background between the tropopause and 30 km (~11 hPa) altitude, in reasonable agreement with Figure 4 (top left). The simulated vertical profiles for December (Figure 4, bottom right) also agrees with SAGE II data as analyzed by *Vernier et al.* [2011]. They detected the volcanic cloud at altitudes higher than 35 km, with its bulk between 26 and 27 km (~21–18 hPa).

3.3. Cross-Equatorial Transport

[24] The simulated volcanic cloud reaches middle and high latitudes through two main transport pathways (Figure 4). While part of the cloud is transported northward through the lower stratosphere (~100 hPa), a portion of the

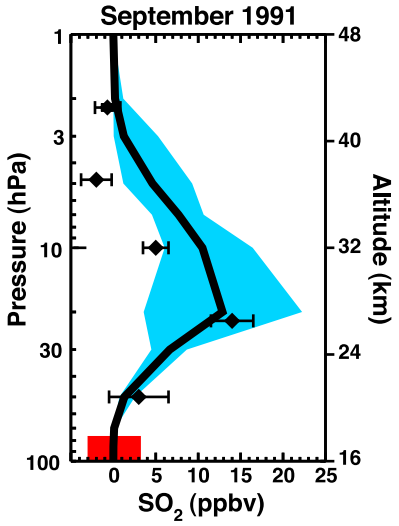

Figure 3. Average vertical profile of the simulated monthly average of the SO_2 mixing ratio (10°S–10°N). The black solid line represents the ensemble average, and the blue shaded area shows the variability of the ensemble REF. The diamonds are Microwave Limb Sounder (MLS) measurements by *Read et al.* [1993]. The red box at the bottom shows the initial injection altitude range.

cloud reaches southern higher latitudes through the middle stratosphere between 5 and 50 hPa. The northward transport is underway within a week of the eruption. The southward transport begins later, and the simulated volcanic cloud arrives at 90°S in the middle of November (Figure 4, bottom). *Hitchman et al.* [1994] inferred the presence of an upper and lower regime from the stratospheric aerosol climatology they derived from satellite data. The simulated volcanic cloud crosses the equator during the first two weeks after the eruption, but the transport from the tropics to southern midlatitudes does not start until the middle of July and becomes significant in September 1991 (Figure 4, top right).

[25] The middle stratospheric transport regime is illustrated in Figure 5. In our simulations the volcanic cloud reaches 30 hPa about one week after the eruption (not shown) and is by then still located in the Northern Hemisphere. At the same time part of the cloud has already reached 40°N and 30°S through the lower stratospheric pathway (not shown). At the beginning of July (Figure 5, top) the volcanic cloud has dispersed longitudinally over nearly the whole globe, but is still confined in the tropical area, with a sharp gradient at 20°S. The same configuration is observed in SAGE II data [*McCormick and Veiga*, 1992; *Trepte et al.*, 1993]. This fast easterly transport, faster than in the observations, is probably due to the easterlies simulated in our runs instead of the different phases of the QBO.

[26] About 1 month after the eruption we simulate the first intrusions of volcanic material from the southern tropics to midlatitudes. The simulated volcanic SO_4 enters the midlatitudes through tongue-like structures in the middle stratosphere (Figure 5, bottom). Such structures have been identified by *Randel et al.* [1993] as the path of mixing from the tropics to midlatitudes. *Trepte et al.* [1993] detected in the SAGE II observations similar intrusions detaching from

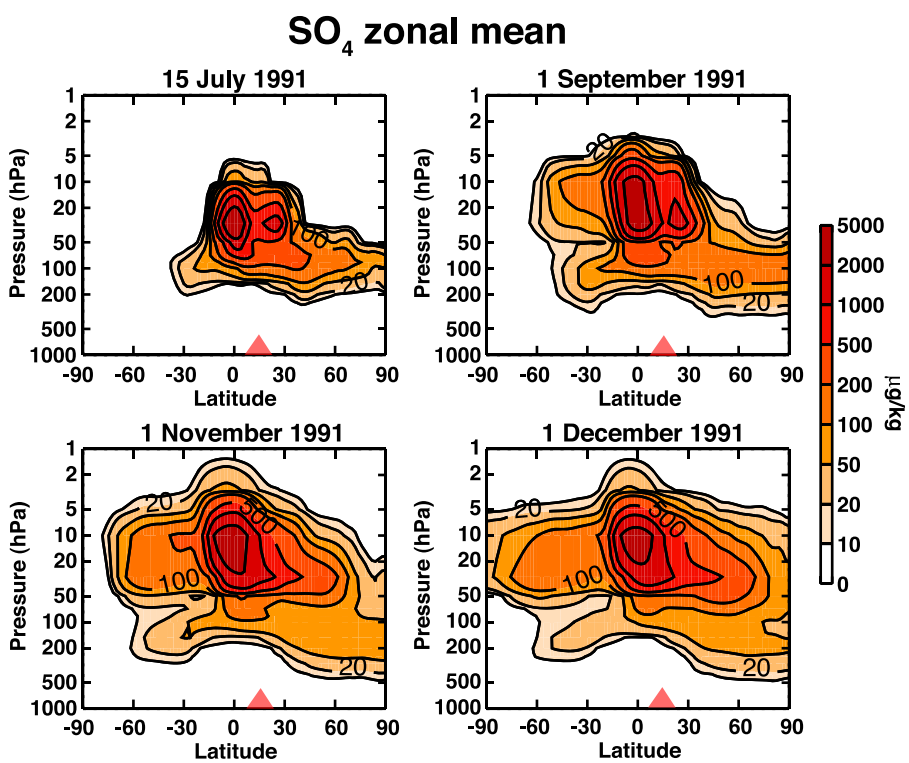

Figure 4. Zonal mean of the simulated SO_4 concentration from Mount Pinatubo (experiment REF) on (top left) 15 July, (top right) 1 September, (bottom left) 1 November, and (bottom right) 31 December 1991.

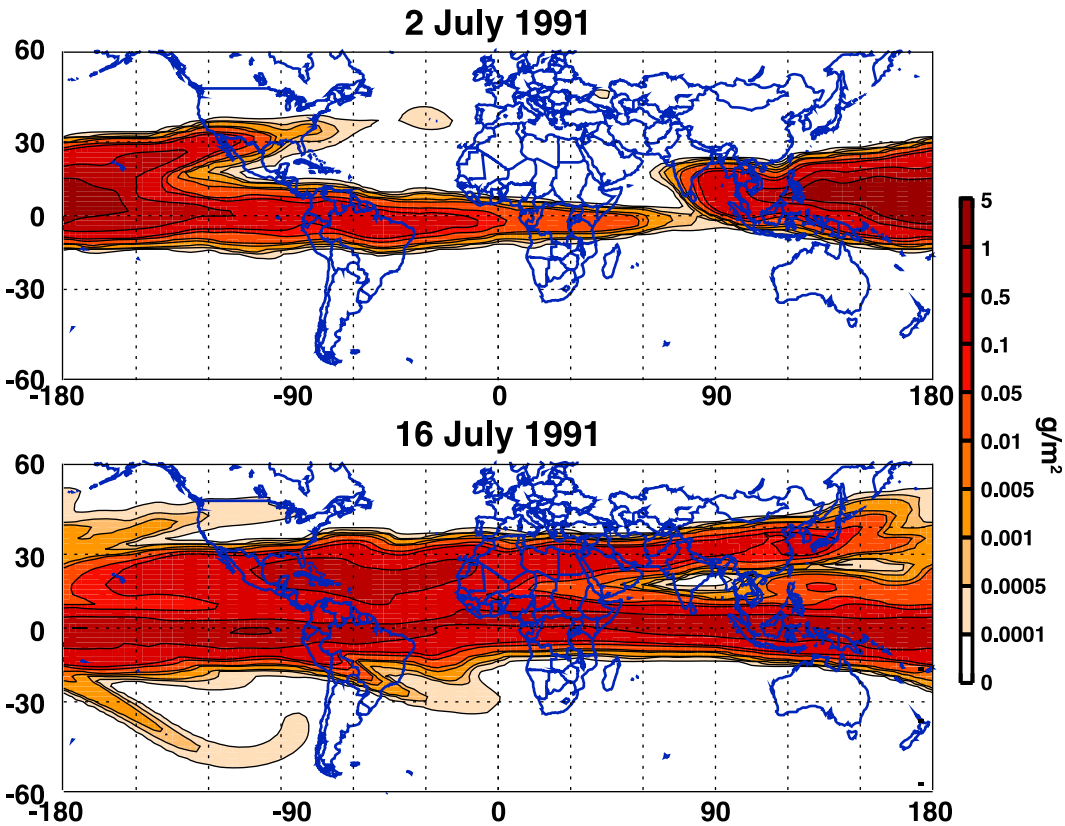

Figure 5. Horizontal distribution of simulated SO_4 column mass (experiment REF) between 30 hPa and the top of the atmosphere on (top) 2 July 1991 and (bottom) 16 July 1991.

the tropical cloud at 20°S between 11 July 1991 and 18 July 1991.

[27] Our transport simulation of the volcanic cloud from the Mount Pinatubo eruption is in good agreement with the observations. Both the vertical and horizontal distribution are similar to the one detected by SAGE II and AVHRR, and also the time scale of the mixing to middle and high latitudes is reasonably close to the observed one.

4. Importance of a Radiatively Active Volcanic Aerosol

[28] We investigate how the interaction between volcanic aerosol from Mount Pinatubo and radiation changed the background mixing within the tropics and from the tropics to midlatitudes. We performed an ensemble of simulations with no interactive aerosol (experiment CONTROL), and compared them to the reference simulation of the dispersal of the volcanic cloud presented in section 3 (experiment REF). Each ensemble member has exactly the same setup of the reference simulations, and is initialized with the same sets of initial conditions.

[29] Figure 6 (top) shows the temporal evolution of the zonally averaged AOT at 550 nm in the experiment CONTROL. Here, most of the volcanic cloud is directed toward the Northern Hemisphere, faster than in the experiment REF (Figure 2, top). This is due to the different vertical distribution of the volcanic cloud: in the experiment CONTROL the volcanic cloud stays at much lower altitudes (Figure 7, middle) than in the experiment REF (Figure 7, left). Hence, the noninteractive cloud of experiment CONTROL does not rise enough to enter the middle stratosphere, and the advection of the cloud to midlatitudes takes place only through the lower stratosphere. The *e*-folding time of SO_4 is much lower in the experiment CONTROL than in the reference case REF (74 days against 346 days).

[30] We also performed an ensemble of three noninteractive simulations directly injecting SO_2 between 17 and 27 km (experiment CONTROL-HIGH). In these simulations the noninteractive SO_2 cloud is injected up to the middle stratosphere. As in the experiment CONTROL, the cross-equatorial transport (Figure 6, bottom) is not as intense as in the reference experiment, and the volcanic cloud looks even more confined to the tropics than in the upper panel of Figure 6. Even if the SO_4 cloud reaches the middle stratosphere (Figure 7, right) and part of the cloud crosses the equator, also in the experiment CONTROL-HIGH the volcanic aerosol remains north of 20°S. The radiative interaction of the volcanic aerosols is therefore essential for a good simulation of the dispersal of the volcanic cloud, as observed by *Timmreck et al.* [1999a].

[31] We are aware that our simulations of the transport of the sulfate cloud from Mount Pinatubo are not complete because of the lack of a QBO in the model version used for this work. However, the influence of the QBO on the aerosol distribution is likely smaller than the perturbation to the stratospheric dynamics induced by an eruption of magnitude like the one of Mount Pinatubo (section 4.1).

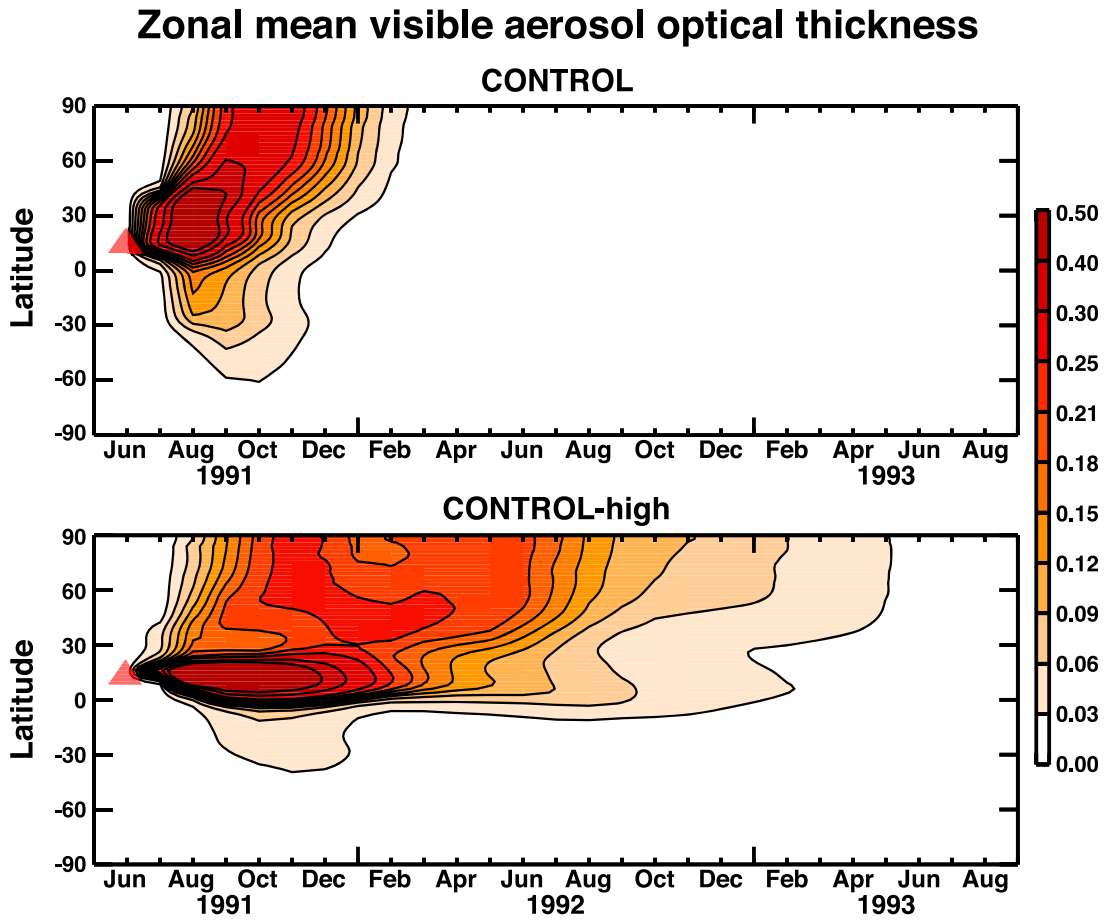

Figure 6. Temporal evolution of the zonally averaged simulated aerosol optical thickness at 550 nm in the ensembles with no radiatively interactive aerosol and SO_2 injection height between (top) 16 and 18 km (experiment CONTROL) and (bottom) 17 and 27 km (experiment CONTROL-HIGH). The red triangle indicates the latitude and time of the Mount Pinatubo eruption.

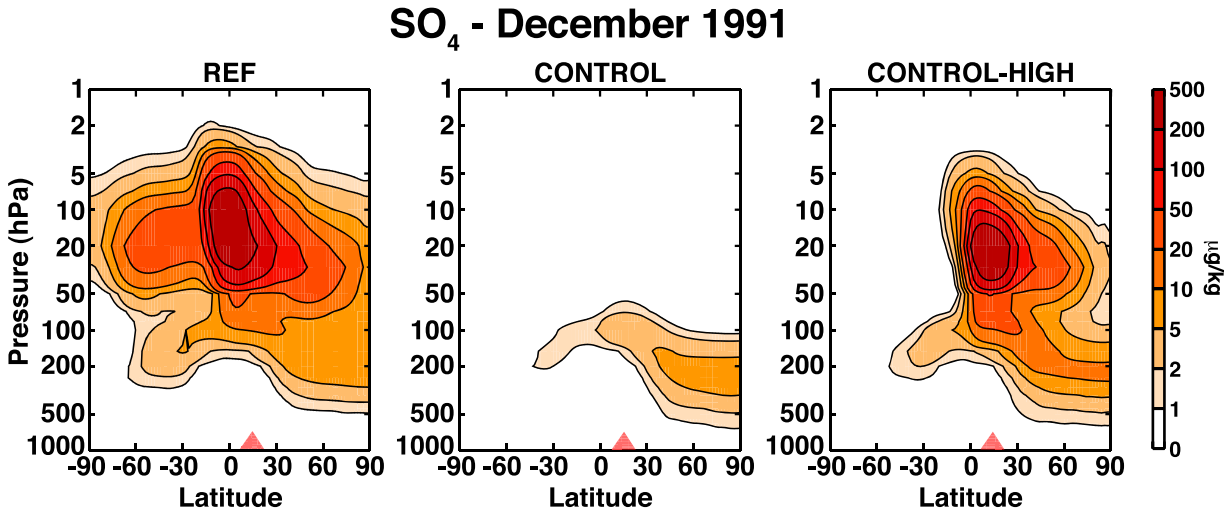

Figure 7. December 1991 monthly mean of the zonally averaged SO_4 concentration in the experiments (left) REF, (middle) CONTROL, and (right) CONTROL-HIGH.

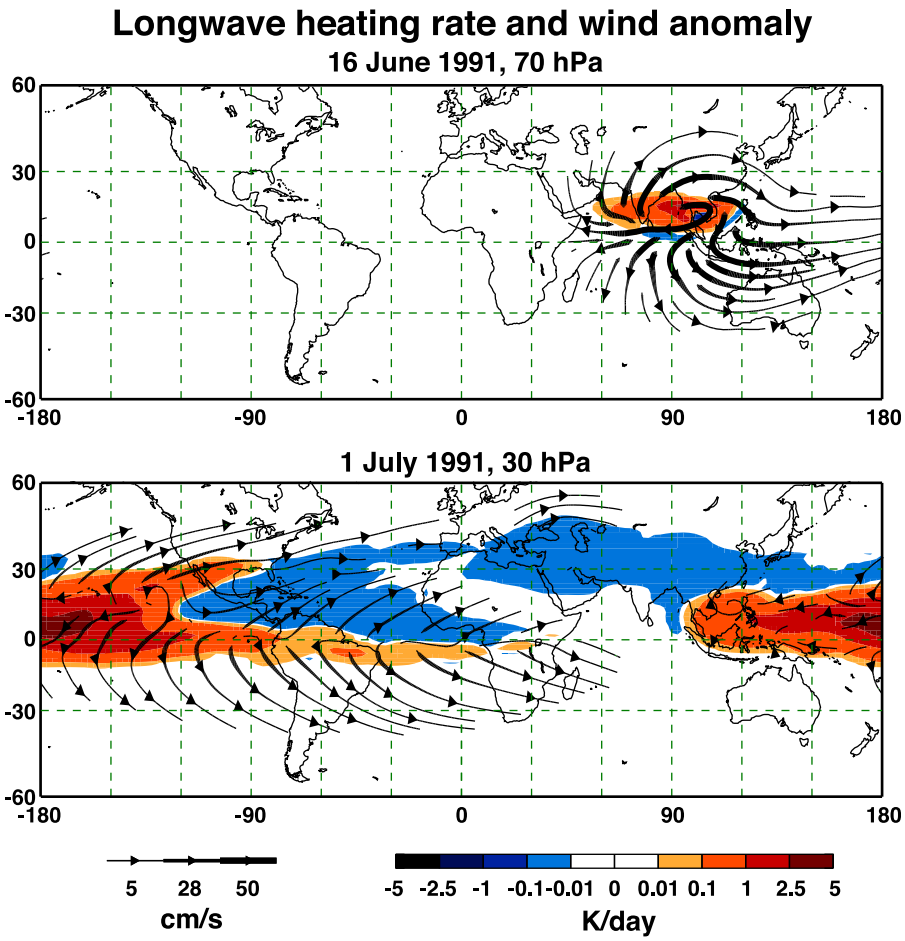

Figure 8. Streamlines of the difference between the horizontal wind field in the interactive (REF) and in the noninteractive (CONTROL) experiments on (top) 16 June 1991 and (bottom) 1 July 1991 at 70 and 30 hPa altitudes, respectively. The shaded areas (nonlinear scale at the bottom) show the heating rates of sulfate from the eruption of Mount Pinatubo due to the interaction with longwave radiation. The wind speed (cm/s) is proportional to the thickness of the streamline contours (see scale at the bottom). Wind speed anomalies of less than 5 cm/s are not plotted.

4.1. Perturbation of the Background Winds

[32] In Figure 8 we show the perturbation of the horizontal winds induced by the interaction between radiation and volcanic aerosol on 16 June 1991 at 70 hPa and on 1 July 1991 at 30 hPa, together with the aerosol heating rates due to longwave radiation. The 16 June perturbation is calculated as the difference of the horizontal winds between the interactive simulations REF and the noninteractive simulations CONTROL. To reduce noise effects, the 1 July perturbation is calculated as the difference of the horizontal winds between the interactive simulations and an ensemble of eight noninteractive simulations initialized on the 00:00 UTC of 1 July 1991 with initial conditions from 1 July 1991 of the REF simulations. This procedure corresponds to running interactive simulations until 30 June 1991, and then switching off the aerosol radiative interaction.

[33] The transient warming due largely to longwave absorption generates a divergent motion from the location of the volcanic cloud already one day after the eruption (Figure 8, top). The simulated volcanic cloud is still at the same latitude as Mount Pinatubo, and has not risen yet to altitudes higher than 50 hPa. Two weeks after the eruption (Figure 8, bottom) the cloud has circled around the whole globe and, in the middle stratosphere, is still confined between 20°S and 20°N. The heating induced by the SO_4 absorption of mainly longwave radiation produces a perturbation of the horizontal winds that diffuses the volcanic cloud to the north toward the tropics and to the south across the equator. By December 1991 the winds at 30 hPa are no longer significantly perturbed. At 50 hPa, where the SO_4 concentration decreases (Figure 4), the winds converge toward the center of the cloud. At altitudes lower than 50 hPa no consistent perturbation is simulated.

[34] GEOS-5 simulates the formation of two anticyclonic vortices near the location of the volcanic cloud during the second week after the eruption, north and south of the equator, respectively (Figure 9). This feature is similar to the response to a tropical tropospheric heating source calculated by *Gill* [1980], with a high-pressure system at the top of the perturbation and a low-pressure one at the bottom.

[35] The divergent winds are strongly related to an increased upwelling. Figure 10 shows the perturbation of the wind's vertical velocity on the same days and levels depicted

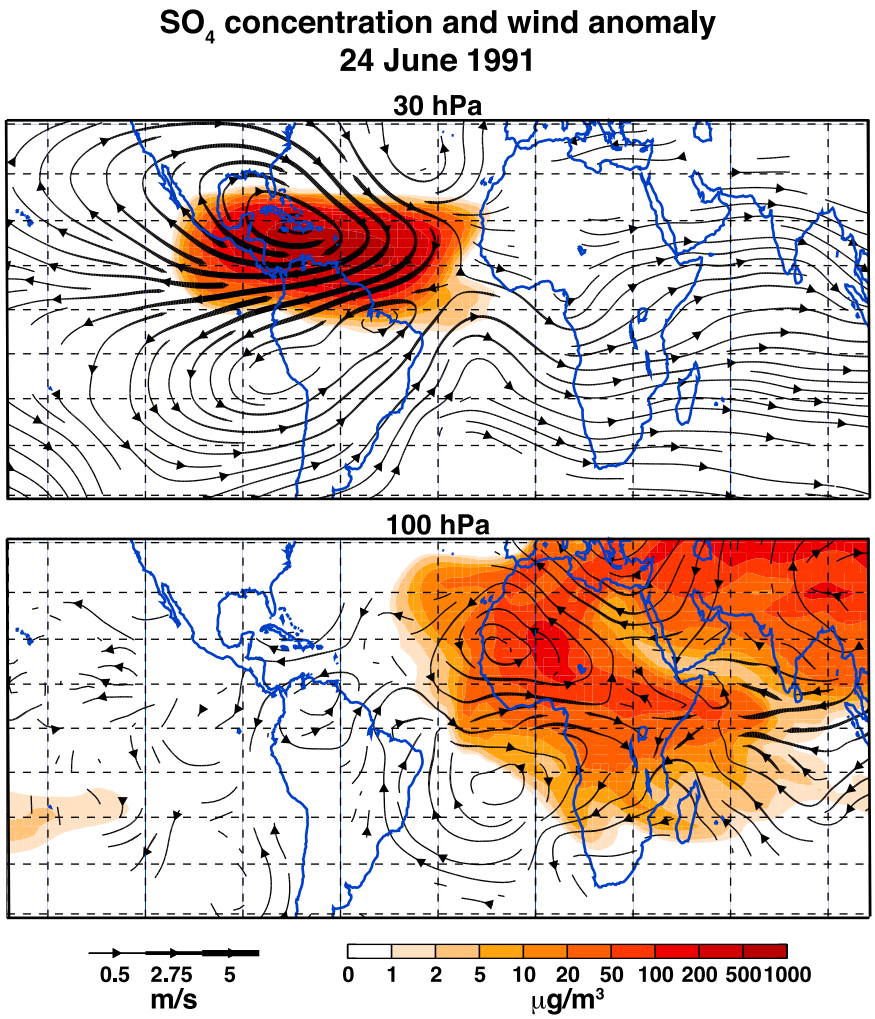

Figure 9. Horizontal distribution of the SO_4 concentration in the experiment REF and streamlines of the perturbation of the horizontal winds (REF-CONTROL) at (top) 30 and (bottom) 100 hPa on 24 June 1991. The wind speed is proportional to the thickness of the streamline contours (see scale at the bottom). Wind speeds of less than 0.5 m/s are not plotted.

in Figure 8, and the contours of the SO_4 distribution. The increase of the vertical velocity is significant: in the non-interactive case the values of the vertical velocity are up to 0.5 mm/s, while in the perturbed case they reach up to 4 mm/s in the regions with highest concentration of sulfate. In some regions the perturbation even changes the sign of the vertical wind. *Fairlie* [1995] also calculated perturbations of the vertical winds up to 4 mm/s.

[36] The absorption of longwave radiation by volcanic SO_4 is largely responsible for the "self-lofting" of the volcanic cloud and for the divergent motion from the areas with highest SO_4 concentration. As already mentioned in section 3.1, the introduction of radiative interactive SO_2 could possibly increase the lofting and the spreading of the cloud during the first months after the eruption.

[37] We can divide the transport of the volcanic cloud to the Southern Hemisphere in two stages: The first stage, driven mainly by the absorption of longwave radiation, comprises the transport from the latitude of the eruption across the equator and to the Southern Hemisphere tropics. The second stage includes the transport of the cloud from the tropics to southern middle and high latitudes through the structures depicted in Figure 5.

[38] We investigated if the volcanic perturbation from Mount Pinatubo enhanced such structures, and hence the mixing between tropics and midlatitudes, by analyzing the distribution of N_2O. Climatologically, the concentration of N_2O is highest in the tropics and presents a strong summer gradient between the tropics and midlatitudes. The sources of N_2O are located at the surface and its concentration decreases with altitude.

[39] Compared to the unperturbed case, GEOS-5 simulates decreased N_2O at about 30 hPa and increased N_2O at 10 hPa in the tropical region starting from September 1991 (Figure 11), compatible with the lofting of air induced by the volcanic perturbation. The effect of the lofting weakens starting from January 1992 and no significant change in the N_2O concentration can be detected after October 1992. There is no sign of increased N_2O transport from the tropics to midlatitudes. This suggests that the radiative perturbation due to the volcanic aerosol did not enhance the mixing between the tropics and midlatitudes in our simulations. The

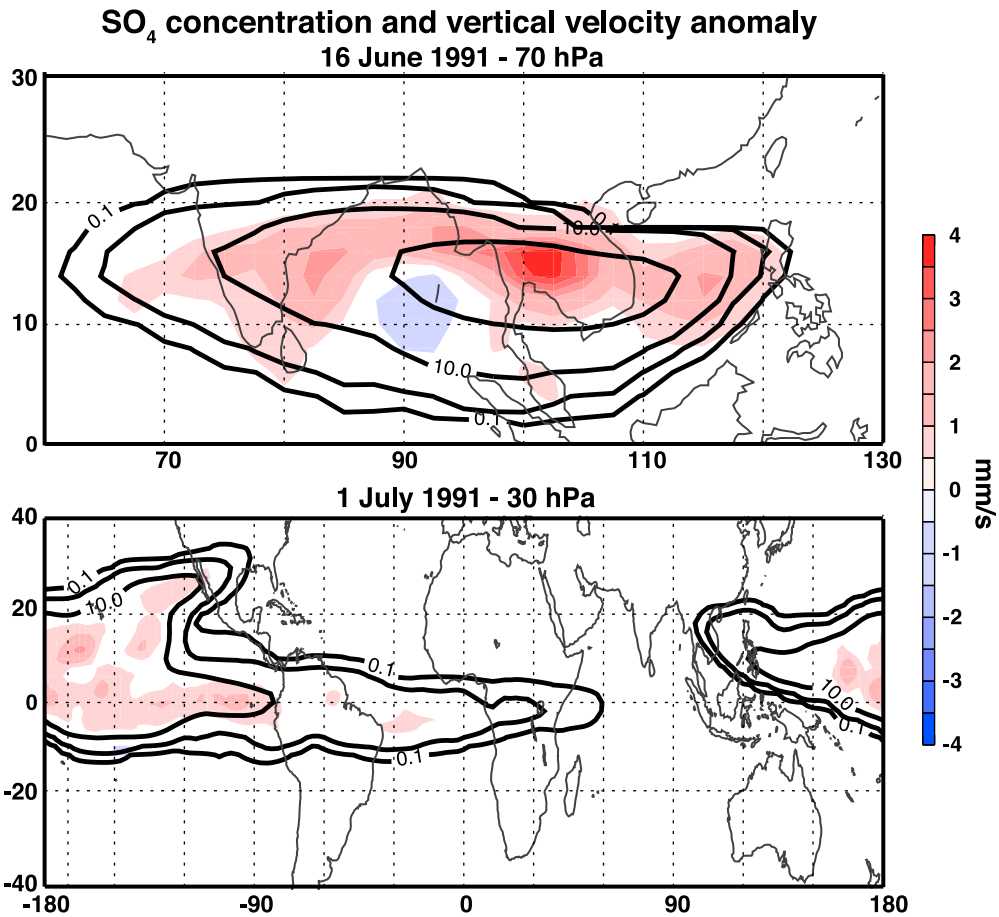

Figure 10. Vertical velocity perturbation (shaded areas) in mm/s (REF-CONTROL) at (top) 70 hPa on 16 June 1991 and (bottom) 30 hPa on 1 July 1991. The contours mark the concentration of SO_4 (in $\mu g/m^3$). The average is calculated over five ensemble members since the needed diagnostic was not available for all the eight ensemble members.

analysis of the age of air at 30 hPa leads to similar conclusion (not shown).

4.2. Impact of the Sulfate Burden on the Spreading of the Volcanic Cloud

[40] We performed two interactive experiments lowering the amount of injected SO_2 to 5 Tg. In the first experiment we injected SO_2 between 16 and 18 km (experiment 0.25REF), in the second between 17 and 27 km (experiment 0.25REF-HIGH). The set up of the simulations is otherwise identical to the reference simulation. Figure 12 shows the vertical profiles of the simulated zonal mean SO_4 on 15 October 1991 in the two experiments. In the experiment with low injection height (Figure 12, left) the volcanic cloud is mainly confined to the lower stratosphere, showing that 5 Tg of SO_2 do not produce a strong enough perturbation to raise the cloud to the middle stratosphere.

[41] In the second experiment (Figure 12, right) the cloud is injected directly in the middle stratosphere and is transported to the Southern Hemisphere through the same middle stratospheric pathway as in the reference simulation. The peak of SO_4, however, is north of the equator, while in the reference simulation the peak is, already on 15 July, partly in the Southern Hemisphere (Figure 4). The cross-equatorial transport is slower in the experiment with low burden than in the reference simulations, but the transport pattern is similar to the one of the reference simulations. The outer edge of the cloud crosses the equator in August 1991 and diffuses

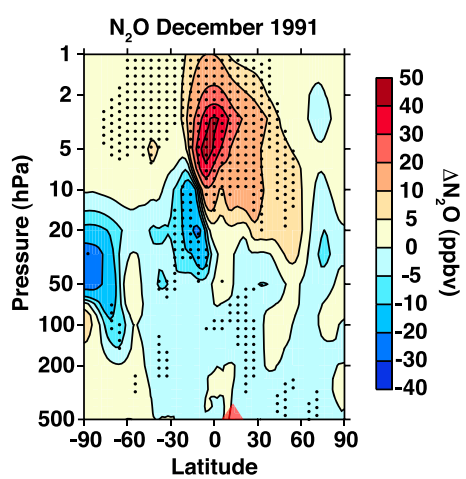

Figure 11. Monthly and zonal mean of the anomaly of the N_2O concentrations in December 1991 (REF-CONTROL). The dotted areas mark regions where the anomaly is significant at 95% level.

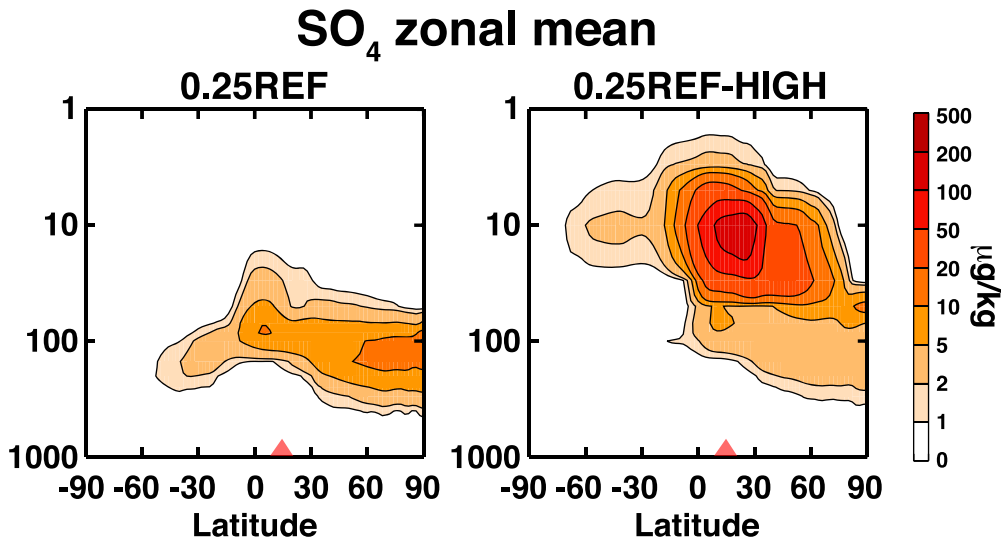

Figure 12. Zonal mean of the SO_4 concentrations on 15 October 1991 in the simulations with low volcanic burden. In these experiments we injected 5 Tg of SO_2 (left) between 16 and 18 km (0.25REF) and (right) between 17 and 27 km (0.25REF-HIGH) at the same time and location of the Mount Pinatubo eruption (denoted as the red triangle).

outside the tropical area starting from October 1991, compared to the end of June 1991 and August 1991, respectively, for experiment REF. This shows that the perturbation induced by the injection of 5 Tg of sulfate is not strong enough to bring the cloud to the middle stratosphere but, if directly injected at that altitude, the cloud is transported anyhow south of the equator and to midlatitudes.

5. Effect of the Eruption Season on the Cross-Equatorial Transport

[42] The Mount Pinatubo and El Chichón volcanic clouds showed significantly different latitude dispersion patterns, with most of the El Chichón cloud remaining in the Northern Hemisphere. In order to understand this difference, we performed two additional Pinatubo-like experiments injecting 20 Tg of SO_2 on 15 January 1991 (experiment WINTER) and on 4 April 1991, the day of the 1982 eruption of El Chichón (experiment SPRING). Each experiment consists of three simulations, initialized on 1 January 1991 with three of the sets of initial condition used for the experiment REF (section 3). These experiments are identical to the reference simulations, except for the SO_2 injection date.

[43] Figure 13 shows the temporal evolution of the zonally averaged AOT in the experiments WINTER, SPRING and REF. In the experiment WINTER (Figure 13, top) the volcanic cloud stays mainly in the Northern Hemisphere, even though it reaches the same altitude as in the experiment REF (not shown). The peak of SO_4 concentration is in the Northern Hemisphere between 10°N and 30°N in March. During the following 4 months the sulfate cloud extends across the equator. The middle stratospheric pathway is present also in this simulation, but is directed toward northern high latitudes, following the direction of the Brewer-Dobson circulation. It is not until June that a small amount of sulfate crosses 30°S and reaches the southern midlatitudes through the middle stratospheric pathway identified in the experiment REF.

[44] In the experiment SPRING (Figure 13, middle) the peak of sulfate aerosol also stays in the Northern Hemisphere, between 0 and 10°N. The edge of the cloud crosses the equator already during the first month, and starts spreading to midlatitudes in June, as in the experiment WINTER and REF. A considerable fraction of the cloud is directed to southern midlatitudes through the middle stratospheric pathway, even more than in the experiment REF (Figure 13, bottom). The difference might be because in June more SO_2 has been converted into SO_4 in the experiments SPRING than in the experiment REF because of the different injection dates.

[45] The season of the eruption alone, therefore, does not appear to be responsible for the difference in transport pattern of the El Chichón and Mount Pinatubo volcanic clouds.

6. Conclusions

[46] We simulate a Mount Pinatubo–like eruption with the free-running general circulation model GEOS-5, coupled to the aerosol transport module GOCART. Our simulations of the transport of the volcanic cloud from the Mount Pinatubo's eruption are in good agreement with observations. By comparing simulations with and without radiative interactive aerosol, we show that including the interaction between radiation and volcanic SO_4 is essential to properly simulate the impact of volcanoes on the atmospheric circulation, as suggested by *Young et al.* [1994] and *Fairlie* [1995].

[47] We can divide the problem of the transport of the Pinatubo aerosol to the Southern Hemisphere in two stages: During the first stage, the absorption of longwave radiation from the cloud induces a lofting and a divergent motion from the center of the cloud. This self-induced transport of the cloud pushes the aerosol northward and southward across the equator and into the SH tropics. The magnitude of the perturbation of the vertical velocity is closely related to the amount and distribution of volcanic SO_4. This perturbation of the tropical circulation persists until December 1991.

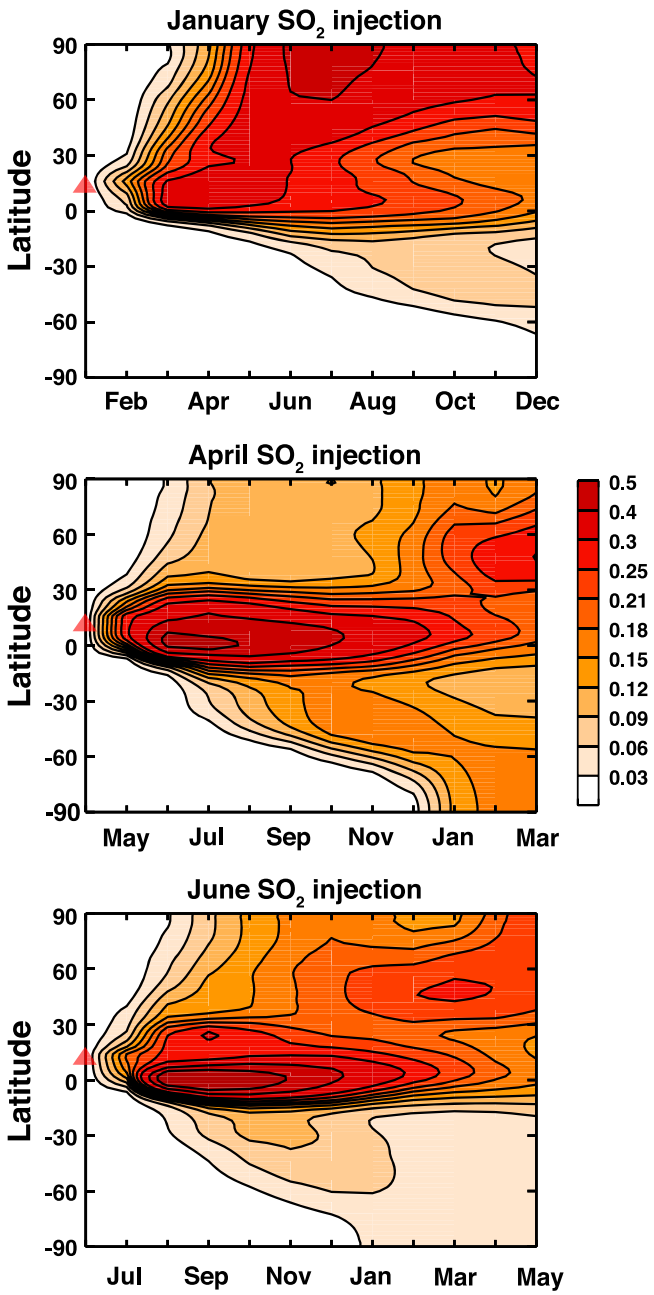

Figure 13. Zonal mean of the visible aerosol optical thickness in the experiments with SO_2 injection on (top) 15 January 1991 (WINTER), (middle) 4 April 1991 (SPRING), and (bottom) 15 June 1991 (REF). Each panel reports the time evolution of the visible aerosol optical thickness during 1 year after the eruption. The red triangles show the latitude and time of the simulated eruption.

During this first stage, the volcanic cloud reaches middle and high latitudes of the Northern Hemisphere through the lower stratosphere at about 100 hPa. In the middle stratosphere the cloud is roughly confined within 20°S and 40°N.

[48] The second stage, starting from about 1 month after the eruption, includes the transport from 30°S to southern middle and high latitudes. Such transport takes place in the middle stratosphere through background structures [*Randel et al.*, 1993]. Analyzing the horizontal distribution of N_2O, we could not detect any significant enhancement of the mixing between tropics and midlatitudes due to the radiative impact of volcanic aerosol.

[49] The transport across the equator of the volcanic cloud from a Mount Pinatubo–like eruption is strongly dependent on the season of the eruption and is much enhanced if the eruption takes place during or just prior to the southern hemispheric winter. The seasonal dependence of the transport, however, does not appear to be responsible for the different transport pattern of the volcanic cloud from Mount Pinatubo and El Chichón.

[50] Our simulations suggest that the difference in the transport of the El Chichón and Mount Pinatubo cloud is more likely related to the amount of SO_2 injected in the atmosphere than to the eruption season. An injected burden equal to 5 Tg SO_2 is not sufficient to take the volcanic cloud to the middle stratosphere and, therefore, to the altitude where the volcanic cloud would be transported to the Southern Hemisphere. El Chichón injected about 7 Tg of SO_2 in the atmosphere [*Bluth et al.*, 1992], which might not have been enough to induce significant lofting to the middle stratosphere.

[51] **Acknowledgments.** We thank Anne Douglass, Steven Pawson, and Chaim Garfinkel for helpful discussions. We also thank three anonymous reviewers, who helped to significantly enhance this paper. V. Aquila is supported by the NASA Postdoctoral Program, administered by the Oak Ridge Associated University (ORAU).

References

Anderson, J., and V. K. Saxena (1996), Evolution of the Mt. Pinatubo aerosol over Antarctica inferred from SAGE II extinction measurements, *Atmos. Environ.*, *30*(10–11), 1797–1804, doi:10.1016/1352-2310(95)00388-6.

Barnes, J. E., and D. J. Hofmann (1997), Lidar measurements of stratospheric aerosol over Mauna Loa Observatory, *Geophys. Res. Lett.*, *24*(15), 1923–1926, doi:10.1029/97GL01943.

Bingen, C., D. Fussen, and F. Vanhellemont (2004), A global climatology of stratospheric aerosol size distribution parameters derived from SAGE II data over the period 1984–2000: 1. Methodology and climatological observations, *J. Geophys. Res.*, *109*, D06201, doi:10.1029/2003JD003518.

Bluth, G. J. S., S. D. Doiron, C. C. Schnetzler, A. J. Krueger, and L. S. Walter (1992), Global tracking of the SO_2 cloud from the June, 1991 Mount Pinatubo eruptions, *Geophys. Res. Lett.*, *19*(2), 151–154, doi:10.1029/91GL02792.

Chin, M., R. B. Rood, S.-J. Lin, and J.-F. Müller (2000), Atmospheric sulfur cycle simulated in the global model GOCART: Model description and global properties, *J. Geophys. Res.*, *105*(D20), 24,671–24,687, doi:10.1029/2000JD900384.

Chin, M., P. Ginoux, S. Kinne, O. Torres, B. Holben, B. Duncan, R. Martin, J. Logan, A. Higurashi, and T. Nakajima (2002), Tropospheric aerosol optical thickness from the GOCART model and comparisons with satellite and Sun photometer measurements, *J. Atmos. Sci.*, *59*(3), 461–483, doi:10.1175/1520-0469(2002)059<0461:TAOTFT>2.0.CO;2.

Chou, M.-D., and M. J. Suarez (1999), A solar radiation parameterization for atmospheric studies, *NASA Tech. Rep., TM-1999-104606*, 50 pp., NASA Goddard Space Flight Cent., Greenbelt, Md.

Chou, M.-D., M. J. Suarez, X.-Z. Liang, and M. M.-H. Yan (2001), A thermal infrared radiation parameterization for atmospheric studies, *NASA Tech. Rep., TM-2001-104606*, 68 pp., NASA Goddard Space Flight Cent., Greenbelt, Md.

Colarco, P., A. Da Silva, M. Chin, and T. Diehl (2010), Online simulations of global aerosol distributions in the NASA GEOS-4 model and comparisons to satellite and ground-based aerosol optical depth, *J. Geophys. Res.*, *115*, D14207, doi:10.1029/2009JD012820.

Crooks, S. A., and L. J. Gray (2005), Characterization of the 11-year solar signal using a multiple regression analysis of the ERA-40 dataset, *J. Clim.*, *18*, 996–1015, doi:10.1175/JCLI-3308.1.

Deshler, T. (2008), A review of global stratospheric aerosol: Measurements, importance, life cycle, and local stratospheric aerosol, *Atmos. Res.*, *90*(2–4), 223–232, doi:10.1016/j.atmosres.2008.03.016.

Fairlie, T. D. (1995), Three-dimensional transport simulations of the dispersal of volcanic aerosol from Mount Pinatubo, *Q. J. R. Meteorol. Soc.*, *121*(528), 1943–1980, doi:10.1002/qj.49712152809.

Gill, A. E. (1980), Some simple solutions for heat-induced tropical circulation, *Q. J. R. Meteorol. Soc.*, *106*(449), 447–462, doi:10.1002/qj.49710644905.

Guo, S., G. Bluth, W. Rose, I. Watson, and A. Prata (2004), Re-evaluation of SO_2 release of the 15 June 1991 Pinatubo eruption using ultraviolet and infrared satellite sensors, *Geochem. Geophys. Geosyst.*, *5*, Q04001, doi:10.1029/2003GC000654.

Hess, M., P. Koepke, and I. Schult (1998), Optical properties of aerosols and clouds: The software package OPAC, *Bull. Am. Meteorol. Soc.*, *79*(5), 831–844, doi:10.1175/1520-0477(1998)079<0831:OPOAAC>2.0.CO;2.

Hitchman, M. H., M. McKay, and C. R. Trepte (1994), A climatology of stratospheric aerosol, *J. Geophys. Res.*, *99*(D10), 20,689–20,700.

Karpechko, A. Y., N. P. Gillett, M. Dall'Amico, and L. J. Gray (2010), Southern Hemisphere atmospheric circulation response to the El Chichón and Pinatubo eruptions in coupled climate models, *Q. J. R. Meteorol. Soc.*, *136*(652), 1813–1822, doi:10.1002/qj.683.

Kirchner, I., G. L. Stenchikov, H.-F. Graf, A. Robock, and J. C. Antuña (1999), Climate model simulation of winter warming and summer cooling following the 1991 Mount Pinatubo volcanic eruption, *J. Geophys. Res.*, *104*(D16), 19,039–19,055, doi:10.1029/1999JD900213.

Koster, R. D., M. J. Suarez, A. Ducharne, M. Stieglitz, and P. Kumar (2000), A catchment-based approach to modeling land surface processes in a general circulation model: 1. Model structure, *J. Geophys. Res.*, *105*(D20), 24,809–24,822, doi:10.1029/2000JD900327.

Lary, J. D., M. Balluch, and S. Bekki (1994), Solar heating rates after a volcanic eruption: The importance of SO_2 absorption, *Q. J. R. Meteorol. Soc.*, *120*, 1683–1688, doi:10.1002/qj.49712052011.

Lin, S.-J. (2004), A "vertically Lagrangian" finite-volume dynamical core for global models, *Mon. Weather Rev.*, *132*, 2293–2307, doi:10.1175/1520-0493(2004)132<2293:AVLFDC>2.0.CO;2.

Lock, A. P., A. R. Brown, M. R. Bush, G. M. Martin, and R. N. B. Smith (2000), A new boundary layer mixing scheme. Part I: Scheme description and single-column model tests, *Mon. Weather Rev.*, *128*, 3187–3199, doi:10.1175/1520-0493(2000)128<3187:ANBLMS>2.0.CO;2.

Long, C. S., and L. L. Stowe (1994), Using the NOAA/AVHRR to study stratospheric aerosol optical thicknesses following the Mt. Pinatubo eruption, *Geophys. Res. Lett.*, *21*, 2215–2218, doi:10.1029/94GL01322.

Louis, J., M. Tiedtke, and J. Geleyn (1982), A short history of the PBL parameterization at ECMWF, paper presented at ECMWF Workshop on Planetary Boundary Layer Parameterization, Eur. Cent. for Medium-Range Weather Forecats, Reading, U. K.

Marshall, G. J. (2003), Trends in the southern annular mode from observations and reanalyses, *J. Clim.*, *16*, 4134–4143, doi:10.1175/1520-0442(2003)016<4134:TITSAM>2.0.CO;2.

McCormick, M. P., and T. J. Swissler (1983), Stratospheric aerosol mass and latitudinal distribution of the El Chichón eruption cloud for October 1982, *Geophys. Res. Lett.*, *10*(9), 877–880, doi:10.1029/GL010i009p00877.

McCormick, M. P., and R. E. Veiga (1992), SAGE-II measurements of early Pinatubo aerosols, *Geophys. Res. Lett.*, *19*(2), 155–158, doi:10.1029/91GL02790.

McCormick, M., L. W. Thomason, and C. R. Trepte (1995), Atmospheric effects of the Mt Pinatubo eruption, *Nature*, *373*, 399–404, doi:10.1038/373399a0.

Moorthi, S., and M. J. Suarez (1992), Relaxed Arakawa-Schubert. A parameterization of moist convection for general circulation models, *Mon. Weather Rev.*, *120*, 978–1002, doi:10.1175/1520-0493(1992)120<0978:RASAPO>2.0.CO;2.

Nagai, T., B. Liley, T. Sakai, T. Shibata, and O. Uchino (2010), Post-Pinatubo evolution and subsequent trend of the stratospheric aerosol layer observed by mid-latitude lidars in both hemispheres, *SOLA*, *6*, 69–72, doi:10.2151/sola.2010-018.

Niemeier, U., C. Timmreck, H. F. Graf, S. Kinne, S. Rast, and S. Self (2009), Initial fate of fine ash and sulfur from large volcanic eruptions, *Atmos. Chem. Phys.*, *9*(22), 9043–9057, doi:10.5194/acp-9-9043-2009.

Pawson, S., R. S. Stolarski, A. R. Douglass, P. A. Newman, J. E. Nielsen, S. M. Frith, and M. L. Gupta (2008), Goddard Earth Observing System chemistry-climate model simulations of stratospheric ozone-temperature coupling between 1950 and 2005, *J. Geophys. Res.*, *113*, D12103, doi:10.1029/2007JD009511.

Petters, M. D., and S. M. Kreidenweis (2007), A single parameter representation of hygroscopic growth and cloud condensation nucleus activity, *Atmos. Chem. Phys.*, *7*(8), 1961–1971, doi:10.5194/acp-7-1961-2007.

Pitts, M. C., and L. W. Thomason (1993), The impact of the eruptions of Mount Pinatubo and Cerro Hudson on Antarctic aerosol levels during the 1991 austral spring, *Geophys. Res. Lett.*, *20*(22), 2451–2454, doi:10.1029/93GL02160.

Randel, W. J., J. C. Gille, A. E. Roche, J. B. Kumer, J. L. Mergenthaler, J. W. Waters, E. F. Fishbein, and W. A. Lahoz (1993), Stratospheric transport from the tropics to middle latitudes by planetary-wave mixing, *Nature*, *365*, 533–535, doi:10.1038/365533a0.

Read, W. G., L. Froidevaux, and J. W. Waters (1993), Microwave Limb Sounder measurement of stratospheric SO2 from the Mt. Pinatubo volcano, *Geophys. Res. Lett.*, *20*(12), 1299–1302, doi:10.1029/93GL00831.

Rienecker, M. M., et al. (2008), The GEOS-5 data assimilation system—Documentation of versions 5.0.1, 5.1.0, and 5.2.0, *NASA Tech. Rep., TM-2008-104606*, 118 pp., NASA Goddard Space Flight Cent., Greenbelt, Md.

Rienecker, M. M., et al. (2011), MERRA: NASA's Modern-Era Retrospective Analysis for Research and Applications, *J. Clim.*, *24*(14), 3624–3648, doi:10.1175/JCLI-D-11-00015.1.

Robock, A. (2000), Volcanic eruptions and climate, *Rev. Geophys.*, *38*(2), 191–219, doi:10.1029/1998RG000054.

Robock, A., T. Adams, M. Moore, L. Oman, and G. Stenchikov (2007), Southern Hemisphere atmospheric circulation effects of the 1991 Mount Pinatubo eruption, *Geophys. Res. Lett.*, *34*, L23710, doi:10.1029/2007GL031403.

Roscoe, H. K., and J. D. Haigh (2007), Influences of ozone depletion, the solar cycle and the QBO on the southern annular mode, *Q. J. R. Meteorol. Soc.*, *133*(628), 1855–1864, doi:10.1002/qj.153.

Russell, P., et al. (1996), Global to microscale evolution of the Pinatubo volcanic aerosol derived from diverse measurements and analyses, *J. Geophys. Res.*, *101*(D13), 18,745–18,763, doi:10.1029/96JD01162.

Saxena, V. K., J. Anderson, and N.-H. Lin (1995), Changes in Antarctic stratospheric aerosol characteristics due to volcanic eruptions as monitored by the Stratospheric Aerosol and Gas Experiment II satellite, *J. Geophys. Res.*, *100*(D8), 16,735–16,751, doi:10.1029/95JD01537.

Stenchikov, G., I. Kirchner, A. Robock, H. Graf, J. Antuña, R. Grainger, A. Lambert, and L. Thomason (1998), Radiative forcing from the 1991 Mount Pinatubo volcanic eruption, *J. Geophys. Res.*, *103*(D12), 13,837–13,857, doi:10.1029/98JD00693.

Stieglitz, M., A. Ducharne, R. Koster, and M. Suarez (2001), The impact of detailed snow physics on the simulation of snow cover and subsurface thermodynamics at continental scales, *J. Hydrometeorol.*, *2*(3), 228–242, doi:10.1175/1525-7541(2001)002<0228:TIODSP>2.0.CO;2.

Thomas, M. A., M. A. Giorgetta, C. Timmreck, H. F. Graf, and G. Stenchikov (2009), Simulation of the climate impact of Mt. Pinatubo eruption using ECHAM5—Part 2: Sensitivity to the phase of the QBO and ENSO, *Atmos. Chem. Phys.*, *9*(9), 3001–3009, doi:10.5194/acp-9-3001-2009.

Thomason, L. W., L. R. Poole, and T. Deshler (1997), A global climatology of stratospheric aerosol surface area density deduced from Stratospheric Aerosol and Gas Experiment II measurements: 1984–1994, *J. Geophys. Res.*, *102*(D7), 8967–8976, doi:10.1029/96JD02962.

Timmreck, C., H. Graf, and I. Kirchner (1999a), A one and half year interactive MA/ECHAM4 simulation of Mount Pinatubo Aerosol, *J. Geophys. Res.*, *104*(D8), 9337–9359, doi:10.1029/1999JD900088.

Timmreck, C., H. Graf, and J. Feichter (1999b), Simulation of Mt. Pinatubo volcanic aerosol with the Hamburg climate model ECHAM4, *Theor. Appl. Climatol.*, *62*(3–4), 85–108, doi:10.1007/s007040050076.

Trepte, C. R., R. E. Veiga, and M. P. McCormick (1993), The poleward dispersal of Mount Pinatubo volcanic aerosol, *J. Geophys. Res.*, *98*(D10), 18,563–18,573, doi:10.1029/93JD01362.

Vernier, J. P., et al. (2011), Major influence of tropical volcanic eruptions on the stratospheric aerosol layer during the last decade, *Geophys. Res. Lett.*, *38*, L12807, doi:10.1029/2011GL047563.

Young, R. E., H. Houben, and O. B. Toon (1994), Radiatively forced dispersion of the Mt. Pinatubo volcanic cloud and induced temperature perturbations in the stratosphere during the first few months following the eruptions, *Geophys. Res. Lett.*, *21*(5), 369–372, doi:10.1029/93GL03302.

Zhao, J., R. P. Turco, and O. B. Toon (1995), A model simulation of Pinatubo volcanic aerosols in the stratosphere, *J. Geophys. Res.*, *100*(D4), 7315–7328, doi:10.1029/94JD03325.

V. Aquila, P. R. Colarco, P. A. Newman, L. D. Oman, and R. S. Stolarski, Atmospheric Chemistry and Dynamics Laboratory, NASA Goddard Space Flight Center, Mail Code 614, Greenbelt, MD 20771, USA. (valentina.aquila@nasa.gov)